Nonminimal quartic inflation in classically conformal U(1)X extended standard model

Nonminimal quartic inflation in classically conformal $U(1)_X$ extended standard model

Satsuki Oda,[1,2] Nobuchika Okada,[3] Digesh Raut,[3] and Dai-suke Takahashi[1,2]

[1]*Okinawa Institute of Science and Technology Graduate University (OIST), Onna, Okinawa 904-0495, Japan*

[2]*Research Institute, Meio University, Nago, Okinawa 905-8585, Japan*

[3]*Department of Physics and Astronomy, University of Alabama, Tuscaloosa, Alabama 35487, USA*

(Received 28 November 2017; published 2 March 2018)

We propose quartic inflation with nonminimal gravitational coupling in the context of the classically conformal $U(1)_X$ extension of the standard model (SM). In this model, the $U(1)_X$ gauge symmetry is radiatively broken through the Coleman-Weinberg mechanism, by which the $U(1)_X$ gauge boson (Z' boson) and the right-handed Majorana neutrinos acquire their masses. We consider their masses in the range of $\mathcal{O}(10\ \mathrm{GeV}) - \mathcal{O}(10\ \mathrm{TeV})$, which are accessible to high-energy collider experiments. The radiative $U(1)_X$ gauge symmetry breaking also generates a negative mass squared for the SM Higgs doublet, and the electroweak symmetry breaking occurs subsequently. We identify the $U(1)_X$ Higgs field with inflaton and calculate the inflationary predictions. Because of the Coleman-Weinberg mechanism, the inflaton quartic coupling during inflation, which determines the inflationary predictions, is correlated to the $U(1)_X$ gauge coupling. With this correlation, we investigate complementarities between the inflationary predictions and the current constraint from the Z' boson resonance search at the LHC Run 2 as well as the prospect of the search for the Z' boson and the right-handed neutrinos at the future collider experiments.

DOI: 10.1103/PhysRevD.97.055001

I. INTRODUCTION

Cosmological inflation [1] provides not only solutions to problems in the standard big bang cosmology, such as the flatness and horizon problems, but also the primordial density fluctuations which are necessary for the formation of the large scale structure observed in the present Universe. In a simple inflationary scenario known as the slow-roll inflation, inflation is driven by a single scalar field (inflaton) while inflaton is slowly rolling down its potential to the minimum. During the slow roll, the inflaton potential energy dominates the energy density of the Universe, and the Universe undergoes an accelerated expansion era, namely, cosmological inflation. The inflation ends when the kinetic energy of inflaton starts dominating over its potential energy, and the inflaton eventually decays into particles in the standard model (SM). The Universe is reheated by relativistic particles created from the inflaton decay and continues to the standard big bang cosmology.

The Planck 2015 results [2] have set an upper bound on the tensor-to-scalar ratio as $r \lesssim 0.1$, while the best fit value for the spectral index (n_s) is 0.9655 ± 0.0062 at 68% C.L. Hence, the chaotic inflation models with simple inflaton (ϕ) potentials such as $V \propto \phi^4$ and $V \propto \phi^2$ are disfavored because of their predictions for r being too large. Among many inflation models, quartic inflation with nonminimal gravitational coupling is a very simple model, which can satisfy the constraints from the Planck 2015 results for a nonminimal gravitational coupling $\xi \gtrsim 0.001$ [3].

In the viewpoint of particle physics, we may think that an inflation model is more compelling if the inflaton also plays an important role in the model. The Higgs inflation scenario [4–6] is a well-known example, in which the SM Higgs field is identified with the inflaton. Also, we may consider a unified scenario between inflaton and the dark matter particle [7]. When the SM is extended with some extra or unified gauge groups, such extensions always include an extra Higgs field in addition to the SM Higgs field, which is necessary to spontaneously break the gauge symmetry down to the SM one. Similarly to the Higgs inflation scenario, we may identify the extra Higgs field with the inflaton.

In this paper, we consider an inflation scenario in the context of the minimal $U(1)_X$ extension of the SM [the minimal $U(1)_X$ model] with the conformal invariance at the classical level [8], where three generations of right-handed neutrinos and a $U(1)_X$ Higgs field are introduced in addition to the SM particle content. The minimal $U(1)_X$

model is a generalization of the well-known minimal $U(1)_{B-L}$ model [9], in which the $U(1)_X$ gauge group is realized as a linear combination of the $B-L$ (baryon number minus lepton number) U(1) and the SM $U(1)_Y$ hypercharge gauge groups [10]. The presence of the three right-handed neutrinos is crucial for cancellation of the gauge and mixed-gravitational anomalies, as well as for incorporating the neutrino masses and flavor mixings into the SM via the seesaw mechanism [11].

Motivated by the argument in Ref. [12] that the classical conformal invariance could be a clue for solving the gauge hierarchy problem, we impose the classically conformal invariance on the minimal $U(1)_X$ model. Although the conformal invariance is broken at the quantum level, we follow the procedure by Coleman and Weinberg [13] and define our model as a massless theory. This model possesses interesting properties: The $U(1)_X$ gauge symmetry is radiatively broken via the Coleman-Weinberg mechanism [13]. Associated with this symmetry breaking, the $U(1)_X$ gauge boson (Z' boson) and the right-handed (Majorana) neutrinos acquire their masses. Through a mixing quartic coupling between the $U(1)_X$ Higgs and the SM Higgs doublet fields, the electroweak symmetry breaking is triggered once the $U(1)_X$ symmetry is radiatively broken.

In the classically conformal $U(1)_X$ model, we consider the quartic inflation with nonminimal gravitational coupling. Here, we identify the $U(1)_X$ Higgs field as the inflaton. Because of the symmetry breaking via the Coleman-Weinberg mechanism, the quartic (self-) coupling of the $U(1)_X$ Higgs field relates to the $U(1)_X$ gauge coupling; in other words, we have a relation between the inflaton mass and the Z' boson mass. Since the inflationary predictions are controlled by the inflaton quartic coupling in the quartic inflation with nonminimal gravitational coupling, we have a correlation between the inflationary predictions and Z' boson physics. Assuming the Z' boson mass in the range of $\mathcal{O}(10\ \mathrm{GeV})$–$\mathcal{O}(10\ \mathrm{TeV})$, we investigate complementarities between the inflationary predictions and the current constraints from the Z' boson resonance search at the Large Hadron Collider (LHC) as well as the prospect of the search for the Z' boson and the right-handed neutrinos at the future collider experiments.

This paper is organized as follows: In the next section, we review the basics of the quartic inflation with nonminimal gravitational coupling and the constraints on the inflationary predictions from the Planck 2015 results. In Sec. III, we present the classically conformal $U(1)_X$ extended SM, and discuss the interesting property of the model, such as the radiative $U(1)_X$ symmetry breaking and the subsequent electroweak symmetry breaking. Identifying the $U(1)_X$ Higgs field as an inflaton, we investigate the quartic inflation with nonminimal gravitational coupling in Sec. IV. Because of the radiative $U(1)_X$ symmetry breaking, the inflaton quartic coupling during inflation relates to the $U(1)_X$ gauge coupling at low energies through the renormalization group evolutions. In Sec. V, we discuss the current collider constraints on the Z' production cross section and the future prospects of the search for the Z' boson and the right-handed neutrinos. Here, we emphasize complementarities between the collider physics and the inflationary predictions. For completion of our inflation scenario, we discuss reheating after inflation in Sec. VI. The last section is devoted to conclusions.

II. NONMINIMAL QUARTIC INFLATION

In this section, we introduce the quartic inflation with nonminimal gravitational coupling (nonminimal quartic inflation). We define the inflation scenario by the following action in the Jordan frame:

$$\mathcal{S}_J = \int d^4x\sqrt{-g}\left[-\frac{1}{2}f(\phi)\mathcal{R}+\frac{1}{2}g^{\mu\nu}(\partial_\mu\phi)(\partial_\nu\phi)-V_J(\phi)\right], \tag{1}$$

where $f(\phi)=(1+\xi\phi^2)$, $V_J(\phi)$ is the scalar potential and the reduced Planck mass, $M_P=2.44\times10^{18}$ GeV, is set to be 1 (Planck unit), ϕ is a real scalar (inflaton), $\xi>0$ is a dimensionless and real parameter of the nonminimal gravitational coupling, and λ is a quartic coupling of the inflaton. In the limit $\xi\to0$, the model is reduced to the minimal quartic inflation.

To obtain an action with a canonically normalized kinetic term for gravity in the so-called Einstein frame, we perform a canonical transformation of the Jordan frame metric, $f(\phi)g_{\mu\nu}=g_{E\mu\nu}$, so that

$$\sqrt{-g}=\frac{1}{f(\phi)^2}\sqrt{-g_E},$$
$$\mathcal{R}=f(\phi)\left(\mathcal{R}_E-\frac{3}{2}(\nabla\ln f(\phi))^2\right). \tag{2}$$

The action in the Einstein frame is then given by

$$S_E=\int d^4x\sqrt{-g_E}\left[-\frac{1}{2}\mathcal{R}_E+\frac{1}{2}\left(\frac{1}{f(\phi)}+\frac{6\xi^2\phi^2}{f(\phi)^2}\right)g_E^{\mu\nu}(\partial_\mu\phi)(\partial_\nu\phi)-\frac{V_J(\phi)}{f(\phi)^2}\right]. \tag{3}$$

Using a field redefinition,

$$\left(\frac{d\sigma}{d\phi}\right)^2 = \frac{1+\xi(6\xi+1)\phi^2}{(1+\xi\phi^2)^2}, \tag{4}$$

the scalar kinetic term is canonically normalized and we obtain

$$S_E = \int d^4x\sqrt{-g_E}\left[-\frac{1}{2}\mathcal{R}_E + \frac{1}{2}g_E^{\mu\nu}(\partial_\mu\sigma)(\partial_\nu\sigma) - V_E(\phi(\sigma))\right], \tag{5}$$

where the inflaton potential in the Einstein frame in terms of the original ϕ is described as[1]

$$V_E = \frac{\lambda}{4}\frac{\phi^4}{(1+\xi\phi^2)^2}. \tag{6}$$

Note that for large $\phi \gg 1/\sqrt{\xi}$, V_E becomes a constant. Hence the potential is suitable for the slow-roll inflation.

We express the slow-roll parameters in terms of ϕ as follows:

$$\begin{aligned}
\epsilon(\phi) &= \frac{1}{2}\left(\frac{V_E'}{V_E\sigma'}\right)^2, \\
\eta(\phi) &= \frac{V_E''}{V_E(\sigma')^2} - \frac{V_E'\sigma''}{V_E(\sigma')^3}, \\
\zeta(\phi) &= \left(\frac{V_E'}{V_E\sigma'}\right)\left(\frac{V_E'''}{V_E(\sigma')^3} - 3\frac{V_E''\sigma''}{V_E(\sigma')^4}\right. \\
&\quad \left. + 3\frac{V_E'(\sigma'')^2}{V_E(\sigma')^5} - \frac{V_E'\sigma'''}{V_E(\sigma')^4}\right),
\end{aligned} \tag{7}$$

where a prime denotes a derivative with respect to ϕ. The amplitude of the curvature perturbation $\Delta_{\mathcal{R}}$ is given by

$$\Delta_{\mathcal{R}}^2 = \left.\frac{V_E}{24\pi^2\epsilon}\right|_{k_0}, \tag{8}$$

which should satisfy $\Delta_{\mathcal{R}}^2 = 2.195\times10^{-9}$ from the Planck measurements [2] with the pivot scale chosen at $k_0 = 0.002\ \mathrm{Mpc}^{-1}$. The number of e-folds is given by

$$N_0 = \frac{1}{\sqrt{2}}\int_{\phi_e}^{\phi_0} d\phi\frac{\sigma'}{\sqrt{\epsilon(\phi)}}, \tag{9}$$

where ϕ_0 is the inflaton value at horizon exit of the scale corresponding to k_0, and ϕ_e is the inflaton value at the end of inflation, which is defined by $\epsilon(\phi_e) = 1$. The value of N_0 depends logarithmically on the energy scale during inflation as well as on the reheating temperature, and we take its typical value to be $N_0 = 50$–60 in order to solve the horizon and flatness problems.

[1]Because of the conformal transformation, the SM interaction terms are also scaled by $1/f(\phi)^2$. However, since $\phi \ll 1$ (in Planck units) at the vacuum, the effect of this higher dimensional operator on SM particles is negligible.

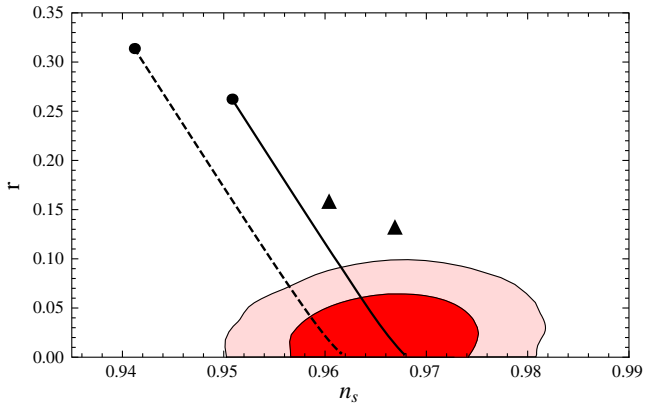

FIG. 1. The inflationary predictions (n_s and r) in the nonminimal quartic inflation for various values of $\xi \geq 0$, along with the contours for the limits at the C.L. of 68% (inner) and 95% (outer) obtained by the Planck measurements (*Planck* TT + lowP + BKP) [2]. The solid and the dashed diagonal lines correspond to the inflationary predictions for $N_0 = 60$ and $N_0 = 50$, respectively. The predictions of the minimal quartic inflation ($\xi = 0$) for $N_0 = 60$ and $N_0 = 50$ are depicted by the right and left black points, respectively. Here, we also show the predictions of the quadratic inflation for $N_0 = 60$ and $N_0 = 50$ as the right and left triangles, respectively. As ξ is increased, the predicted r values approach their asymptotic values $r \simeq 0.00296$ and 0.00419 for $N_0 = 60$ and $N_0 = 50$, respectively.

The slow-roll approximation is valid as long as the conditions $\epsilon \ll 1$, $|\eta| \ll 1$, and $\zeta \ll 1$ hold. In this case, the inflationary predictions, the scalar spectral index n_s, the tensor-to-scalar ratio r, and the running of the spectral index $\alpha = \frac{dn_s}{d\ln k}$ are given by

$$n_s = 1 - 6\epsilon + 2\eta, \qquad r = 16\epsilon, \qquad \alpha = 16\epsilon\eta - 24\epsilon^2 - 2\zeta. \tag{10}$$

Here, the inflationary predictions are evaluated at $\phi = \phi_0$. Under the constraint of $\Delta_{\mathcal{R}}^2 = 2.195\times10^{-9}$ from the Planck measurements [2], once N_0 is fixed, all the inflationary predictions as well as the quartic coupling λ are determined as a function of ξ. In Fig. 1, we show the inflationary predictions (n_s and r) for various values of $\xi \geq 0$, along with the contours for the limits at the C.L. of 68% (inner) and 95% (outer) obtained by the Planck measurements (*Planck* TT + lowP + BKP) [2]. The solid and the dashed diagonal lines correspond to the inflationary predictions for $N_0 = 60$ and $N_0 = 50$, respectively. The predictions of the minimal quartic inflation ($\xi = 0$) for $N_0 = 60$ and $N_0 = 50$ are depicted by the right and left black points, respectively. Here, we also show the predictions of the quadratic inflation for $N_0 = 60$ and $N_0 = 50$ as the right and left triangles, respectively. As ξ is increased, the inflationary predictions approach their

TABLE I. Inflationary predictions for various values of ξ in the nonminimal quartic inflation for fixed $N_0 = 60$ and 50. Here, ϕ_0 and ϕ_e are evaluated in the Planck units ($M_P = 1$).

$N_0 = 60$						
ξ	ϕ_0	ϕ_e	n_s	r	$\alpha(10^{-4})$	λ
0	22.1	2.83	0.951	0.262	−8.06	1.43×10^{-13}
0.003 33	22.00	2.79	0.961	0.1	−7.03	3.79×10^{-13}
0.0689	18.9	2.30	0.967	0.01	−5.44	6.69×10^{-12}
1	8.52	1.00	0.968	0.00346	−5.25	4.62×10^{-10}
10	2.89	0.337	0.968	0.00301	−5.24	4.01×10^{-8}
100	0.920	0.107	0.968	0.00297	−5.23	3.95×10^{-6}
1000	0.291	0.0340	0.968	0.00296	−5.23	3.94×10^{-4}
$N_0 = 50$						
ξ	ϕ_0	ϕ_e	n_s	r	$\alpha(10^{-4})$	λ
0	20.2	2.83	0.941	0.314	−11.5	2.45×10^{-13}
0.005 27	20.0	2.77	0.955	0.1	−9.74	7.83×10^{-13}
0.119	15.8	2.07	0.961	0.01	−7.70	1.96×10^{-11}
1	7.82	1.00	0.961	0.00489	−7.51	6.56×10^{-10}
10	2.65	0.337	0.962	0.00426	−7.49	5.70×10^{-8}
100	0.844	0.107	0.962	0.00420	−7.48	5.61×10^{-6}
1000	0.267	0.0340	0.962	0.004 19	−7.48	5.60×10^{-4}

asymptotic values, $n_s \simeq 0.968$, $\simeq 0.002\,96$, and $\alpha \simeq -5.23 \times 10^{-4}$ for $N_0 = 60$ ($n_s \simeq 0.962$, $r \simeq 0.00419$, and $\alpha \simeq -7.48 \times 10^{-4}$ for $N_0 = 50$). In Fig. 1, we find a lower bound on $\xi \geq 0.00385$, which corresponds to $r \leq 0.0913$ for $N_0 = 60$, from the limit at 95% C.L. We have summarized in Table I the numerical values of the inflationary predictions for various ξ values and fixed $N_0 = 60$ and 50.

III. CLASSICALLY CONFORMAL $U(1)_X$ EXTENDED STANDARD MODEL

The model we investigate is the minimal $U(1)_X$ extension of the SM with classically conformal invariance [8], which is based on the gauge group $SU(3)_c \times SU(2)_L \times U(1)_Y \times U(1)_X$. The particle content of the model is listed in Table II. In addition to the SM particle content, three generations of right-hand neutrinos (RHNs) N_R^i and a $U(1)_X$ Higgs field Φ are introduced. In the following, the real part of the scalar Φ is identified with the inflaton. The $U(1)_X$ gauge group is defined as a linear combination of the SM $U(1)_Y$ and the $U(1)_{B-L}$ gauge groups, and hence the $U(1)_X$ charges of fields are determined by two real parameters, x_H and x_Φ. Since the charge x_Φ always appears as a product with the $U(1)_X$ gauge coupling, it is not an independent free parameter of the model, and hence we fix $x_\Phi = 1$ throughout this paper. We reproduce the minimal $B - L$ model as the limit of $x_H \to 0$. The limit of $x_H \to +\infty(-\infty)$ indicates that the $U(1)_X$ is (anti-) aligned to the SM $U(1)_Y$ direction. The anomaly structure of the model is the same as the minimal $B - L$ model [9], and all the gauge

TABLE II. The particle content of the minimal $U(1)_X$ extended SM. In addition to the SM particle content ($i = 1, 2, 3$), the three right-handed neutrinos [N_R^i ($i = 1, 2, 3$)] and the $U(1)_X$ Higgs field (Φ) are introduced. The $U(1)_X$ charge of a field is determined by two real parameters, x_H and x_Φ, as $Q_X = Y x_H + Q_{BL} x_\Phi$ with its hypercharge (Y) and $B - L$ charge (Q_{BL}). Without loss of generality, we fix $x_\Phi = 1$ throughout this paper.

	$SU(3)_c$	$SU(2)_L$	$U(1)_Y$	$U(1)_X$
q_L^i	**3**	**2**	1/6	$(1/6)x_H + (1/3)x_\Phi$
u_R^i	**3**	**1**	2/3	$(2/3)x_H + (1/3)x_\Phi$
d_R^i	**3**	**1**	−1/3	$(-1/3)x_H + (1/3)x_\Phi$
ℓ_L^i	**1**	**2**	−1/2	$(-1/2)x_H + (-1)x_\Phi$
e_R^i	**1**	**1**	−1	$(-1)x_H + (-1)x_\Phi$
H	**1**	**2**	−1/2	$(-1/2)x_H$
N_R^i	**1**	**1**	0	$(-1)x_\Phi$
Φ	**1**	**1**	0	$(+2)x_\Phi$

and mixed-gravitational anomalies are canceled in the presence of the three RHNs. The covariant derivative relevant to the $U(1)_Y \times U(1)_X$ gauge interaction is given by

$$D_\mu = \partial_\mu - i(g_1 Y + \tilde{g} Q_X) B_\mu - i g_X Q_X Z'_\mu, \tag{11}$$

where in addition to the $U(1)_Y$ gauge coupling (g_1) and the $U(1)_X$ gauge coupling (g_X), a new gauge coupling $\tilde{g}$ is introduced from a kinetic mixing between the two U(1) gauge bosons. For simplicity, we set $\tilde{g} = 0$ at the $U(1)_X$ symmetry breaking scale. Although nonzero $\tilde{g}$ is generated in its renormalization group evolution toward high energies, we find that its effect on our final results is negligible.

The Yukawa sector of the SM is extended to have

$$\mathcal{L}_{\text{Yukawa}} \supset -\sum_{i=1}^{3}\sum_{j=1}^{3} Y_D^{ij} \bar{\ell}_L^i H N_R^j - \frac{1}{2}\sum_{k=1}^{3} Y_M^k \Phi \bar{N}_R^{kC} N_R^k + \text{H.c.}, \tag{12}$$

where the first and the second terms are the neutrino Dirac Yukawa couplings and the Majorana Yukawa couplings, respectively. Without loss of generality, the Majorana Yukawa couplings are already diagonalized in our basis. Once the $U(1)_X$ Higgs field Φ develops nonzero vacuum expectation value (VEV), the $U(1)_X$ gauge symmetry is broken and the Majorana masses for the RHNs are generated. Then, the light neutrino masses are generated via the seesaw mechanism [11] after the electroweak symmetry breaking. In this paper, we consider the degenerate mass spectrum for the RHNs, $Y_M^1 = Y_M^2 = Y_M^3 \equiv Y_M$, for simplicity.

Since we impose the classically conformal invariance on the minimal $U(1)_X$ model, the renormalizable scalar potential at the tree level is given by

$$V = \lambda_H (H^\dagger H)^2 + \lambda_\Phi (\Phi^\dagger \Phi)^2 - \lambda_{\rm mix} (H^\dagger H)(\Phi^\dagger \Phi), \quad (13)$$

where all quartic couplings are chosen to be positive. Note that the mass terms for the SM Higgs doublet (H) and the $U(1)_X$ Higgs (Φ) are forbidden by the conformal invariance. In the following, we assume that $\lambda_{\rm mix}$ is negligibly small (this is justified later), and analyze the Higgs potential separately for Φ and H as a good approximation.

Let us first analyze the $U(1)_X$ Higgs sector. At the one-loop level, the Coleman-Weinbeg potential [13] is calculated to be

$$V(\phi) = \frac{\lambda_\Phi}{4}\phi^4 + \frac{\beta_\Phi}{8}\phi^4\left(\ln\left[\frac{\phi^2}{v_\phi^2}\right] - \frac{25}{6}\right), \quad (14)$$

where $\phi/\sqrt{2} = \Re[\Phi]$ is a real scalar, and we have chosen the renormalization scale as the VEV of Φ ($\langle\phi\rangle = v_\phi$). The stationary condition $dV/d\phi|_{\phi=v_\phi} = 0$ leads to a relation,

$$\lambda_\Phi = \frac{11}{6}\beta_\Phi, \quad (15)$$

between the renormalized self-coupling defined as

$$\lambda_\Phi = \frac{1}{3!}\frac{d^4V(\phi)}{d\phi^4}\bigg|_{\phi=v_\phi} \quad (16)$$

and the coefficient of the one-loop corrections,[2]

$$\beta_\Phi = \frac{1}{16\pi^2}(20\lambda_\Phi^2 + 96g_X^4 - 3Y_M^4) \simeq \frac{1}{16\pi^2}(96g_X^4 - 3Y_M^4). \quad (17)$$

Here, we have used $\lambda_\Phi^2 \ll g_X^4$ in the last expression. Note that the $U(1)_X$ symmetry breaking via the Coleman-Weinberg mechanism relates the $U(1)_X$ Higgs quartic coupling to the gauge and Majorana Yukawa couplings in Eq. (15). The vacuum stability requires $Y_M < (32)^{1/4} g_X$.

We next consider the SM Higgs sector. In our model, the electroweak symmetry breaking is achieved in a very simple way. Once the $U(1)_X$ symmetry is radiatively broken, the SM Higgs doublet mass is generated through the mixing quartic term in Eq. (13),

$$V \supset \frac{\lambda_H}{4}h^4 - \frac{\lambda_{\rm mix}}{4}v_\phi^2 h^2, \quad (18)$$

where we have replaced H by $H = 1/\sqrt{2}(0h)^T$ in the unitary gauge. As a result, the electroweak symmetry is broken. Here, we emphasize a crucial difference from the SM, namely, the electroweak symmetry breaking is triggered by the radiative $U(1)_X$ gauge symmetry breaking [14], not by a negative mass squared added by hand. The SM Higgs boson mass (m_h) is given by

$$m_h^2 = \lambda_{\rm mix} v_\phi^2 = 2\lambda_H v_h^2, \quad (19)$$

where $v_h = 246$ GeV is the SM Higgs VEV. Considering the Higgs boson mass of $m_h = 125$ GeV [15] and the LEP constraint on $v_\phi \gtrsim 10$ TeV [16–19], we find $\lambda_{\rm mix} \lesssim 10^{-4}$ and the smallness of $\lambda_{\rm mix}$ is justified.

Associated with the $U(1)_X$ and the electroweak symmetry breakings, the $U(1)_X$ gauge boson (Z' boson) and the (degenerate) Majorana RHNs acquire their masses as

$$m_{Z'} = \sqrt{(2g_X v_\phi)^2 + (x_H g_X v_h)^2} \simeq 2g_X v_\phi, \quad m_N = \frac{Y_M}{\sqrt{2}}v_\phi. \quad (20)$$

The $U(1)_X$ Higgs boson mass is given by

$$m_\phi^2 = \frac{d^2V}{d\phi^2}\bigg|_{\phi=v_\phi} = \beta_\Phi v_\phi^2 \simeq \frac{1}{16\pi^2}(96g_X^4 - 3Y_M^4)v_\phi^2 = \frac{6}{\pi}\alpha_X m_{Z'}^2\left(1 - 2\left(\frac{m_N}{m_{Z'}}\right)^4\right), \quad (21)$$

where $\alpha_X = g_X^2/(4\pi)$. The vacuum stability, in other words, $m_\phi^2 > 0$, requires $m_{Z'} > 2^{1/4} m_N$.

IV. NONMINIMAL QUARTIC INFLATION WITH THE $U(1)_X$ HIGGS FIELD

Now we identify the $U(1)_X$ Higgs field with the inflaton in the nonminimal quartic inflation. In the original Jordan frame action, we introduce the nonminimal gravitational coupling of

$$-\xi(\Phi^\dagger\Phi)\mathcal{R}, \quad (22)$$

which leads to the nonminimal gravitational coupling in Eq. (1) for the inflaton/Higgs field defined as $\phi = \sqrt{2}\Re[\Phi]$. The scalar potential in Eq. (1) is replaced by the effective potential in Eq. (14). Since the inflaton value $\phi \gg v_\phi$ during inflation, we can neglect the effects of the VEV v_ϕ for the nonminimal coupling as well as the inflaton potential. In our inflation analysis, we employ the renormalization group (RG) improved effective potential of the form [20],

$$V(\phi) = \frac{1}{4}\lambda_\Phi(\phi)\phi^4, \quad (23)$$

where $\lambda(\phi)$ is the solution to the RG equation with identifying the renormalization scale as ϕ along the inflation trajectory.

[2]In a more precise formulation of the Coleman-Weinberg effective potential, β_Φ includes a $\lambda_{\rm mix}$ term which we have neglected because it is negligibly small compared to the dominant contribution from g_X^4. Also, we define our inflaton trajectory along the ϕ direction with $H = 0$. Hence, even for $\lambda_{\rm mix} \gg \lambda_\Phi$, we can neglect the $\lambda_{\rm mix}$ term in our inflationary analysis.

As we have discussed in Sec. II, the inflationary predictions are determined by the parameter ξ of the nonminimal gravitational coupling. From the viewpoint of the unitarity arguments [21] of the nonminimal quartic inflation scenario, we may take $\xi \lesssim 10$ to make our analysis valid. This means from Table I that the inflaton quartic coupling is very small, $\lambda \lesssim 4 \times 10^{-8}$, for $N_0 = 60$. Note that the stationary condition of Eq. (15) derived from the Coleman-Weinberg mechanism requires the quartic coupling to be very small. Hence, one may consider it natural to realize the nonminimal quartic inflation with a small ξ in the context of our classically conformal model. Because of the stationary condition and $\lambda_\Phi \ll 1$, the $U(1)_X$ gauge and the Majorana Yukawa couplings must be very small, g_X, $Y_M \ll 1$. Thus, the RG evolutions of all couplings in our model are very mild, and we calculate the inflationary predictions with a constant quartic coupling, $\lambda_\Phi(\phi_0)$, evaluated at the inflaton value $\phi = \phi_0$. Our results for the inflationary predictions in the nonminimal quartic inflation are presented in Sec. II. In the following analysis, we identify λ in Sec. II with $\lambda = \lambda_\Phi(\phi_0)$.

We evaluate the inflaton quartic coupling at $\phi = \phi_0$ by extrapolating the gauge, the Majorana Yukawa, and the Higgs quartic couplings at v_ϕ through their RG equations. Since all couplings are very small, the RG equations at the one-loop level are approximately given by

$$\begin{aligned}
\frac{d\lambda_\Phi}{d\ln\phi} &= \beta_\lambda \simeq 96\alpha_X^2 - 3\alpha_Y^2, \\
\frac{d\alpha_X}{d\ln\phi} &= \beta_g = \frac{72 + 64x_H + 41x_H^2}{12\pi}\alpha_X^2, \\
\frac{d\alpha_Y}{d\ln\phi} &= \beta_Y = \frac{1}{2\pi}\alpha_Y\left(\frac{5}{2}\alpha_Y - 6\alpha_X\right),
\end{aligned} \tag{24}$$

where $\alpha_Y = Y_M^2/(4\pi)$. In the leading-log approximation, we have the solutions of the RG equations for α_X and α_Y as

$$\alpha_X(\phi) \simeq \overline{\alpha_X} + \overline{\beta_g}\ln\left[\frac{\phi}{v_\phi}\right], \qquad \alpha_Y(\phi) \simeq \overline{\alpha_Y} + \overline{\beta_Y}\ln\left[\frac{\phi}{v_\phi}\right], \tag{25}$$

where $\overline{\alpha_X} \equiv \alpha_X(v_\phi)$, $\overline{\alpha_Y} \equiv \alpha_Y(v_\phi)$, and $\overline{\beta_g}$ and $\overline{\beta_Y}$ are the beta functions in Eq. (24) evaluated with $\overline{\alpha_X}$ and $\overline{\alpha_Y}$. Using these solutions, we obtain

$$\beta_\lambda \simeq 96\alpha_X^2 - 3\alpha_Y^2 \simeq \overline{\beta_\lambda} + 2(96\overline{\alpha_X}\,\overline{\beta_g} - 3\overline{\alpha_Y}\,\overline{\beta_Y})\ln\left[\frac{\phi}{v_\phi}\right], \tag{26}$$

where $\overline{\beta_\lambda} = 96\overline{\alpha_X} - 3\overline{\alpha_Y}$. Finally, we arrived at an approximate solution as

$$\begin{aligned}
\lambda_\Phi(\phi) &\simeq \overline{\lambda_\Phi} + \overline{\beta_\lambda}\ln\left[\frac{\phi}{v_\phi}\right] + (96\overline{\alpha_X}\,\overline{\beta_g} - 3\overline{\alpha_Y}\,\overline{\beta_Y})\left(\ln\left[\frac{\phi}{v_\phi}\right]\right)^2 \\
&= \left(\frac{11}{6} + \ln\left[\frac{\phi}{v_\phi}\right]\right)\overline{\beta_\lambda} + (96\overline{\alpha_X}\,\overline{\beta_g} - 3\overline{\alpha_Y}\,\overline{\beta_Y})\left(\ln\left[\frac{\phi}{v_\phi}\right]\right)^2,
\end{aligned} \tag{27}$$

where $\overline{\lambda_\Phi} \equiv \lambda_\Phi(v_\phi)$, and we have used Eq. (15) in the second line.

In the next section, we discuss the collider physics for the Z' boson and the heavy Majorana neutrinos. For our discussion, it is convenient to adopt the Z' boson mass ($m_{Z'}$) and the degenerate heavy Majorana neutrino mass (m_N) as free parameters, instead of the $U(1)_X$ Higgs VEV v_ϕ and $\overline{Y_M}$. In our analysis, we have five free parameters,

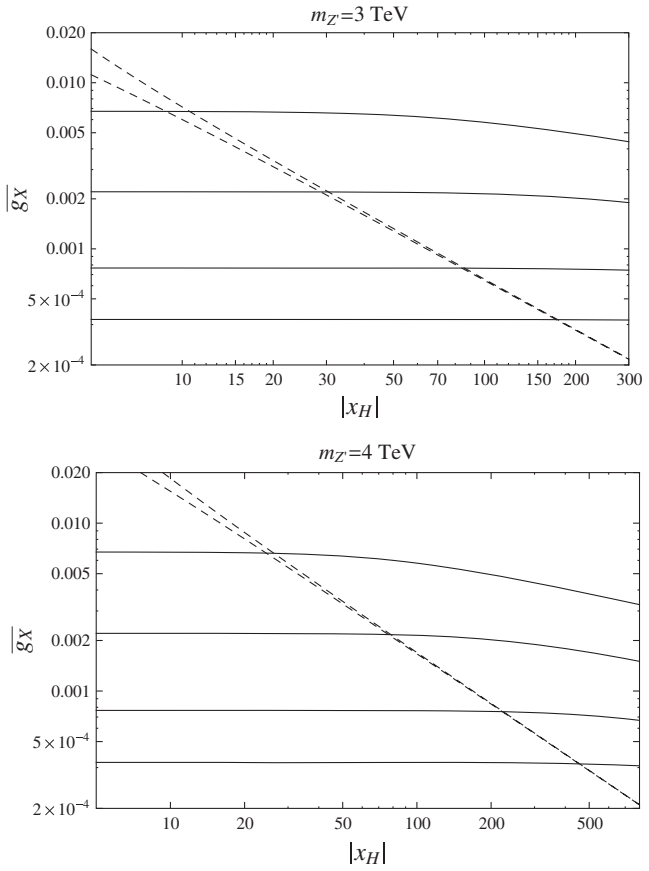

FIG. 2. Left panel: The horizontal solid lines depict the $U(1)_X$ gauge coupling $\overline{g_X}$ as a function of x_H for various values of $\xi = 10$, 1, 0.0689, and 0.00333 from top to bottom, along which the nonminimal quartic inflation is realized. Here, we have fixed $m_{Z'} = 3m_N = 3$ TeV. The result of solid lines for $x_H > 0$ and $x_H < 0$ are well overlapped and indistinguishable. The dashed lines show the upper bounds on $\overline{g_X}$ as a function of x_H from the ATLAS results on the search for a narrow resonance [22]. The upper and lower dashed lines correspond to $x_H < 0$ and $x_H > 0$, respectively. Right panel: same as the left panel, but for $m_{Z'} = 3m_N = 4$ TeV.

namely, ξ, x_H, $\overline{g_X}$, $m_{Z'}$, and m_N, after replacing v_ϕ and $\overline{Y_M}$ by using the relations, $v_\phi = m_{Z'}/(2\overline{g_X})$ and $\overline{Y_M} = \sqrt{2}m_N/v_\phi = 2\sqrt{2}\overline{g_X}(m_N/m_{Z'})$. As has been discussed in Sec. II, once ξ is fixed, not only the inflationary predictions but also ϕ_0, ϕ_e, and $\lambda_\Phi(\phi_0)$ are all determined. When ξ, $m_{Z'}$, and m_N values are fixed, we obtain $\overline{g_X}$ as a function of x_H from Eq. (27). In Fig. 2, we show $\overline{g_X}$ as a function of x_H for various values of ξ for $m_{Z'} = 3$ TeV (left panel) and 4 TeV (right panel). In each panel, the horizontal solid lines correspond to $\xi = 10$, 1, 0.0689, and 0.003 33 from top to bottom. Here, we have fixed $m_N = m_{Z'}/3$ (see the next section), for simplicity. The results for $x_H > 0$ and $x_H < 0$ are well overlapped and indistinguishable.

V. COMPLEMENTARITY BETWEEN COLLIDER PHYSICS AND INFLATION

Realizing the nonminimal quartic inflation in the context of the classically conformal $U(1)_X$ model, we have obtained a relation between the $U(1)_X$ gauge coupling and the inflationary predictions once x_H, $m_{Z'}$, and m_N are fixed. If $m_{Z'} \lesssim 10$ TeV, the Z' boson in our $U(1)_X$ model can be produced at the high-energy colliders. Since the production cross section of the Z' boson depends on its mass, the gauge coupling, and x_H, we have in our model a correlation between the collider physics on the Z' boson and the inflationary predictions.

Let us first consider the LHC phenomenology on the Z' boson. The ATLAS and CMS Collaborations have been searching for a narrow resonance with dilepton final states at the LHC Run 2 [23,24]. In their analysis, the so-called sequential SM Z' (Z'_{SSM}) has been considered as a reference, assuming the Z'_{SSM} boson has exactly the same properties as the SM Z boson, except for its mass. In the following, we interpret the current LHC constraints on the Z'_{SSM} boson into the $U(1)_X$ Z' boson to identify an allowed parameter region. In our analysis, we employ the latest upper bound on the Z'_{SSM} production cross section reported by the ATLAS Collaboration [22].

The cross section for the process $pp \to Z' + X \to \ell^+\ell^- + X$ is given by

$$\sigma = \sum_{q,\bar{q}} \int dM_{\ell\ell} \int_{\frac{M^2_{\ell\ell}}{s}}^1 dx \frac{2M_{\ell\ell}}{xs} f_q(x, Q^2) f_{\bar{q}} \times \left(\frac{M^2_{\ell\ell}}{xs}, Q^2\right) \hat{\sigma}(q\bar{q} \to Z' \to \ell^+\ell^-), \quad (28)$$

where $M_{\ell\ell}$ is the invariant mass of a final state dilepton, f_q is the parton distribution function for a parton (quark) "q," and $\sqrt{s} = 13$ TeV is the center-of-mass energy of the LHC Run 2. In our numerical analysis, we employ CTEQ6L [25] for the parton distribution functions with the factorization scale $Q = m_{Z'}$. The cross section for the colliding partons is given by

$$\hat{\sigma}(q\bar{q} \to Z' \to \ell^+\ell^-) = \frac{\pi}{1296}\overline{\alpha_X}^2 \frac{M^2_{\ell\ell}}{(M^2_{\ell\ell} - m^2_{Z'})^2 + m^2_{Z'}\Gamma^2_{Z'}} F_{q\ell}(x_H), \quad (29)$$

where the functions $F_{q\ell}(x_H)$ are

$$F_{u\ell}(x_H) = (8 + 20x_H + 17x_H^2)(8 + 12x_H + 5x_H^2),$$
$$F_{d\ell}(x_H) = (8 - 4x_H + 5x_H^2)(8 + 12x_H + 5x_H^2), \quad (30)$$

with q being the up-type (u) and down-type (d) quarks, respectively. Since the RG running effect from $m_{Z'}$ to v_ϕ is negligible, we use $\overline{\alpha_X} = \overline{g_X}^2/(4\pi)$ for the $U(1)_X$ gauge coupling in our collider physics analysis. Neglecting the mass of all SM fermions, the total decay width of the Z' boson is given by

$$\Gamma_{Z'} = \frac{\overline{\alpha_X}}{6} m_{Z'} \left[F(x_H) + 3\left(1 - \frac{4m_N^2}{m_{Z'}^2}\right)^{\frac{3}{2}} \theta\left(\frac{m_{Z'}}{m_N} - 2\right)\right] \quad (31)$$

with $F(x_H) = 13 + 16x_H + 10x_H^2$.

In interpreting the latest ATLAS results [22] on the Z'_{SSM} boson in the $U(1)_X$ Z' boson case, we follow the strategy in Ref. [26]: we first calculate the cross section of the process $pp \to Z'_{SSM} + X \to \ell^+\ell^- + X$, and then we scale our result by a k factor so as to match with the theoretical prediction of the cross section presented in the ATLAS paper [22]. With the k factor determined in this way, we calculate the cross section for the process $pp \to Z' + X \to \ell^+\ell^- + X$ to identify an allowed region for the model parameters of $\overline{g_X}$, x_H, and $m_{Z'}$.

In Fig. 2, the dashed lines show the upper bounds on $\overline{g_X}$ as a function of x_H from the ATLAS results on the search for a narrow resonance with the combined dielectron and dimuon channels [22]. The upper and lower dashed lines correspond to $x_H < 0$ and $x_H > 0$, respectively. As we can see in the cross section formula, the dashed lines approach each other for a large $|x_H|$. Combining the ATLAS constraints with the horizontal lines from the inflationary analysis, we find upper bounds on $x_H \lesssim 10$, 30, 80, and 170 for $m_{Z'} = 3$ TeV ($x_H \lesssim 25$, 80, 220, and 450 for $m_{Z'} = 4$ TeV), corresponding to $\xi = 10$, 1, 0.0689, and 0.003 33, respectively. Recall that the inflaton quartic coupling is extremely small for $\xi \lesssim 10$ (see Table I), and this indicates that the $U(1)_X$ gauge coupling is also very small [see Eq. (27)]. Nevertheless, as has been pointed out in Ref. [27], the Z' boson with mass of $\mathcal{O}(1$ TeV) can still be tested at the LHC Run 2 when the $U(1)_X$ gauge symmetry is oriented to the SM $U(1)_Y$ hypercharge direction, namely, $|x_H| \gg 1$.

As the Z' boson is heavier, the current LHC bounds become weaker, because of the energy dependence of the parton distribution functions. We can see this fact by comparing the dashed lines in the left and right panels of Fig. 2. When we take $m_{Z'} = 5$ TeV, which is the

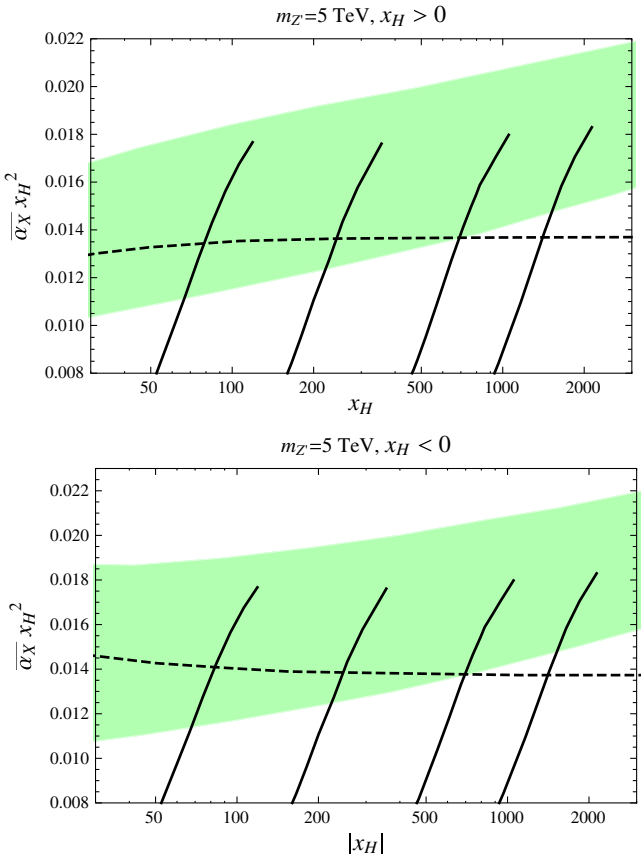

FIG. 3. Left panel: the combined result for $m_{Z'} = 5$ TeV and $x_H > 0$. The shaded (green) region depicts the parameters to resolve the electroweak vacuum instability, while satisfying the perturbativity of the gauge coupling at M_P. The dashed line denotes the upper bound from the ATLAS results for the Z' boson search at the LHC Run 2. The diagonal lines correspond to $\xi = 10$, 1, 0.0689, and 0.00333 from left to right, along which the nonminimal quartic inflation is realized. Right panel: same as the left panel, but for $x_H < 0$.

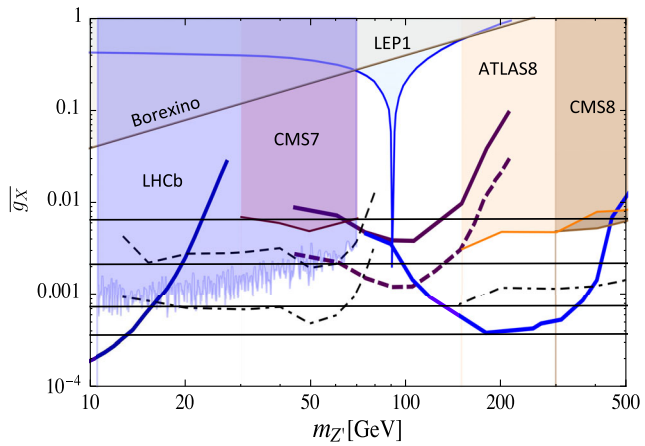

FIG. 4. The $B - L$ gauge coupling ($\overline{g_X}$) as a function of $m_{Z'}$, along with the results presented in Ref. [29]. We also show the current bound from the LHCb results [32]. The horizontal lines correspond to our results for $\xi = 10$, 1, 0.0689, and 0.00333 from top to bottom, respectively, along which the nonminimal quartic inflation is realized. According to the analysis in Ref. [29], we have fixed $m_N = m_{Z'}/3$. The shaded regions are excluded by the indicated experiments. The projected reach of the proposed searches for a Z' boson production and its decay into a pair of RHNs are shown in thick (solid and dashed) curves. The thin (black) curves show the projected sensitivity of direct searches for the Z' boson production via its decay $Z' \to \ell^+\ell^-$ from the LHC Run 1 (dashed), and the high-luminosity LHC (dot-dashed). See Ref. [29] for more details.

maximum Z' boson mass in the ATLAS analysis [22], another interesting parameter region of our model opens up. In Ref. [8], the same model presented in this paper has been investigated in the viewpoint of the electroweak vacuum stability. As is well known, the SM Higgs potential becomes unstable at high energies, since the running SM Higgs quartic coupling runs into the negative region at the renormalization scale of $\mu \simeq 10^{10}$ GeV [28]. It has been shown in Ref. [8] that this electroweak vacuum instability problem can be solved in the context of the classically conformal $\mathrm{U}(1)_X$ model with $\overline{\alpha_X} x_H^2 \gtrsim 0.01$. It is interesting to combine our inflation analysis with the results in Ref. [8].

Figure 3 shows the combined results in the $(x_H, \overline{\alpha_X} x_H^2)$ plane. In the left panel, the parameter region to resolve the electroweak vacuum instability is shown as the shaded (green) region for $m_{Z'} = 5$ TeV and $x_H > 0$. In order to solve the instability problem, $\overline{\alpha_X} x_H^2 \gtrsim 0.01$ is necessary, while $\overline{\alpha_X}$ has an upper bound for a fixed x_H from the requirement $\alpha_X(M_P) < 1$ that the running $\mathrm{U}(1)_X$ gauge coupling is in the perturbative regime at $\mu = M_P$. The dashed line denotes the upper bound from the ATLAS results. The diagonal lines correspond to $\xi = 10$, 1, 0.0689, and 0.003 33 from left to right, along which the nonminimal quartic inflation is realized. Since we have found that the leading-log approximation for the RG analysis is not sufficiently reliable for $\overline{\alpha_X} x_H^2 \gtrsim 0.01$, we have numerically integrated the RG equations in this analysis. See Ref. [8] for details of our RG analysis. The upper bounds on $\overline{\alpha_X} x_H^2 \lesssim 0.018$ shown on the diagonal lines are also from the requirement of $\alpha_X(\phi_0) < 1$ for a given ξ. Since $\phi_0 > M_P$ for $\xi \lesssim 10$, the requirement of $\alpha_X(\phi_0) < 1$ is more severe than that of $\alpha_X(M_P) < 1$. We find the allowed parameter region for $\xi \gtrsim 0.0689$ and $x_H \lesssim 700$, although it is very narrow. The right panel is the same as the left panel, but for $x_H < 0$.

Even if the $\mathrm{U}(1)_X$ gauge coupling is very small and $|x_H| \lesssim 1$, we can test our model when the Z' boson is light, say, $m_{Z'} \lesssim 500$ GeV. In Ref. [29], the authors have considered the RHN production at the high-luminosity LHC [30] and the SHiP [31] experiments in the contest of the minimal $B - L$ model [the limit of $x_H = 0$ in our $\mathrm{U}(1)_X$ model], where a pair of RHNs is created through the decay of a Z' boson resonantly produced at the colliders.

When the RHNs have the mass of $\mathcal{O}(100\ \mathrm{GeV})$ or less, it is long lived and its decay to the SM particles provides a clean signature with a displaced vertex. It has been found in Ref. [29] that for a fixed $m_N = m_{Z'}/3$, the high-luminosity LHC and the SHiP experiments can explore the $B-L$ gauge coupling up to $\overline{g_X} \gtrsim 10^{-4}$ for $10\ \mathrm{GeV} \lesssim m_{Z'} \lesssim 500\ \mathrm{GeV}$. In the $B-L$ limit of $x_H = 0$, we show in Fig. 4 the $B-L$ gauge coupling ($\overline{g_X}$) as a function of $m_{Z'}$, along with the results presented in Ref. [29]. In Fig. 4, we have added the current bound from the LHCb results [32]. The horizontal lines correspond to our results for $\xi = 10, 1, 0.0689$, and 0.003 33 from top to bottom, respectively, along which the nonminimal quartic inflation is realized. Our results very weakly depend on $m_{Z'}$ in the mass range shown in Fig. 4, as can be understood from Eq. (27).

VI. INFLATON MASS AND REHEATING AFTER INFLATION

To complete our inflation scenario, we finally discuss reheating after inflation through the inflaton decay into the SM particles. Since the inflaton is much lighter than the Z' boson and the RHNs in our scenario with $\xi \lesssim 10$, it decays mainly into the SM fermions through the mixing with the SM Higgs boson.

From the Higgs potential in Eq. (13) with the radiative corrections in Eq. (14), we find the following mass matrix for the inflaton (ϕ) and the SM Higgs boson (h) at the potential minimum:

$$\mathcal{L} \supset -\frac{1}{2}\begin{bmatrix} h & \phi \end{bmatrix}\begin{bmatrix} m_h^2 & -m_{\mathrm{mix}}^2 \\ -m_{\mathrm{mix}}^2 & m_\phi^2 \end{bmatrix}\begin{bmatrix} h \\ \phi \end{bmatrix}, \tag{32}$$

where $m_{\mathrm{mix}}^2 = \lambda_{\mathrm{mix}} v_h v_\phi$, $m_h = 125\ \mathrm{GeV}$ and m_ϕ is given in Eq. (21). As can be seen in Sec. III, $m_{\mathrm{mix}}^2, m_\phi^2 \ll m_h^2$ and the mass matrix is almost diagonal. We define the mass eigenstates, ϕ_1 and ϕ_2, by

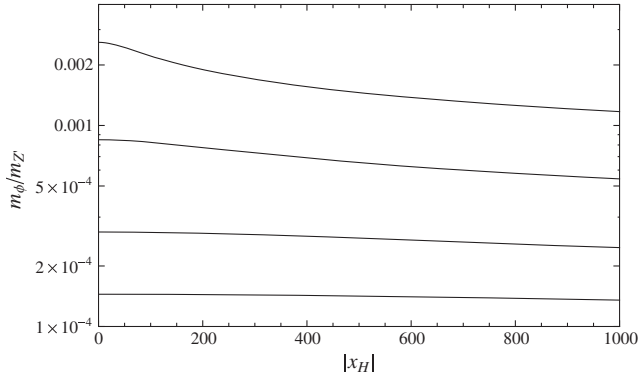

FIG. 5. The mass ratio of $m_\phi/m_{Z'}$ as a function of x_H for $\xi = 10$, 1, 0.0689, and 0.00333 from top to bottom. Although we have used $m_{Z'} = 3$ TeV as a reference, we obtain almost identical results for other values of $m_{Z'}$.

$$\begin{bmatrix} h \\ \phi \end{bmatrix} = \begin{bmatrix} \cos\theta & -\sin\theta \\ \sin\theta & \cos\theta \end{bmatrix}\begin{bmatrix} \phi_1 \\ \phi_2 \end{bmatrix}, \tag{33}$$

with a small mixing angle

$$\theta \simeq \frac{m_{\mathrm{mix}}^2}{m_h^2} = 2\overline{g_X}\left(\frac{v_h}{m_{Z'}}\right) \ll 1. \tag{34}$$

Since the mixing angle is very small, the mass eigenstate ϕ_1 (ϕ_2) is almost the SM Higgs boson [the $\mathrm{U}(1)_X$ Higgs boson].

Through the mixing angle, the inflaton decays into the SM particles. We evaluate the inflaton decay width as

$$\Gamma_\phi \simeq \theta^2 \times \Gamma_h(m_\phi), \tag{35}$$

where $\Gamma_h(m_\phi)$ is the SM Higgs boson decay width if the SM Higgs boson mass were m_ϕ. From Eqs. (21) and (34),

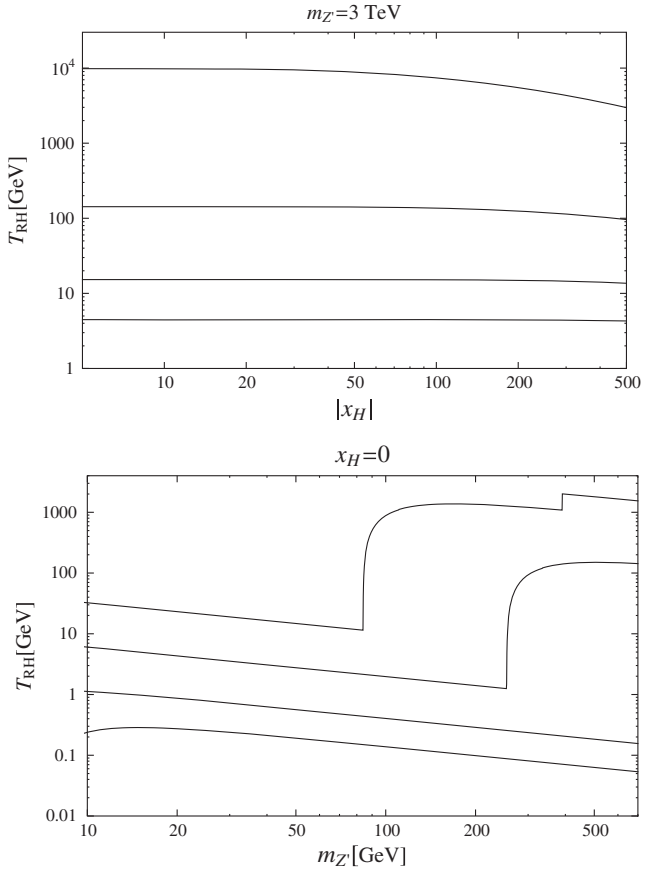

FIG. 6. Reheating temperature after inflation. Left panel: reheating temperature as a function of x_H for $\xi = 10$, 1, 0.0689, and 0.00333 from top to bottom, with $m_{Z'} = 3$ TeV. The results for $x_H > 0$ and $x_H < 0$ are well overlapped and indistinguishable. Right panel: reheating temperature as a function of $m_{Z'}$ in the $B-L$ model ($x_H = 0$). The solid lines correspond to the results for $\xi = 10$, 1, 0.0689, and 0.00333 from top to bottom. Sharp rises of the reheating temperature for threshold values of $m_{Z'}$ imply that new decay channels are opened.

the inflaton mass and its decay width is a function of $\overline{\alpha_X}$ and $m_{Z'}$ (with $m_N = m_{Z'}/3$). For the successful nonminimal inflation, $\overline{\alpha_X}$ is determined as a function of ξ, x_H, and $m_{Z'}$, and hence the inflaton mass and the decay width are controlled by the three parameters, ξ, x_H, and $m_{Z'}$. With the inflaton decay width, we estimate reheating temperature by

$$T_{\rm RH} = \left(\frac{90}{\pi^2 g_*}\right)^{1/4} \sqrt{\Gamma_\phi M_P} \simeq \sqrt{\Gamma_\phi M_P}, \tag{36}$$

where g_* is the total effective degrees of freedom of thermal plasma.

In Fig. 5, we show the ratio of $m_\phi/m_{Z'}$ as a function of x_H for $\xi = 10$, 1, 0.0689, and 0.00333 from top to bottom. The results for $x_H > 0$ and $x_H < 0$ are well overlapped and indistinguishable. Although we have used $m_{Z'} = 3$ TeV as a reference, we find that the result is almost independent of $m_{Z'}$, as we have seen in Fig. 4 with $x_H = 0$. The resultant mass ratios are also weakly depending on x_H.

In Fig. 6, we show the estimated reheating temperature after inflation. The left panel depicts the reheating temperature as a function of x_H for $\xi = 10$, 1, 0.0689, and 0.003 33 from top to bottom, with $m_{Z'} = 3$ TeV. For the $B - L$ limit of $x_H = 0$, the right panel depicts the results as a function of $m_{Z'}$. The solid lines from top to bottom correspond to the results for $\xi = 10$, 1, 0.0689, and 0.003 33, respectively. Sharp rises of the reheating temperature for threshold values of $m_{Z'}$ imply that new decay channels are opened. For example, in the plot for $\xi = 10$, a new decay channel of $\phi \to \mu^+\mu^-$ opens at $m_{Z'} \simeq 80$ GeV. All results presented in Fig. 6 satisfy the model-independent lower bound on reheating temperature, $T_{\rm RH} \gtrsim 1$ MeV, for the successful big bang nucleosynthesis.

VII. CONCLUSIONS

The nonminimal quartic inflation is a simple and successful inflation scenario, and its inflationary predictions are consistent with the Planck 2015 results for the nonminimal gravitational coupling with $\xi \gtrsim 0.003$ for $N_0 = 60$. This inflation scenario would be more compelling if the inflaton plays essential roles for not only inflation but also particle physics phenomena. In many models beyond the SM where the gauge symmetry of the SM is extended, a new Higgs field to break the extended gauge symmetry is commonly introduced. It is an interesting possibility to identify such a Higgs field with the inflaton in the nonminimal quartic inflation.

In this paper, we have considered the classically conformal $\mathrm{U}(1)_X$ extended SM, where the $\mathrm{U}(1)_X$ gauge group is realized as a linear combination of the $\mathrm{U}(1)_{B-L}$ and the SM $\mathrm{U}(1)_Y$ gauge groups. This model has an interesting property that all the gauge symmetry breakings in the model originate from the Coleman-Weinberg mechanism: The $\mathrm{U}(1)_X$ gauge symmetry is radiatively broken through the Coleman-Weinberg mechanism, and this breaking generates a negative mass squared for the SM Higgs doublet and hence, the electroweak symmetry breaking occurs subsequently. Associated with the $\mathrm{U}(1)_X$ gauge symmetry breaking, the Z' boson and the right-handed neutrinos acquire their masses. We have set their masses in the range of $\mathcal{O}(10\ \mathrm{GeV}) - \mathcal{O}(10\ \mathrm{TeV})$, which is accessible at high energy collider experiments.

We have investigated the nonminimal inflation scenario in the context of this classically conformal $\mathrm{U}(1)_X$ model by identifying the $\mathrm{U}(1)_X$ Higgs field with the inflaton. In this model, the $\mathrm{U}(1)_X$ gauge symmetry is radiatively broken through the Coleman-Weinberg mechanism, due to which the inflaton quartic coupling is determined by the $\mathrm{U}(1)_X$ gauge coupling. Since the inflationary predictions in the nonminimal quartic inflation are determined by the inflaton quartic coupling during inflation, we have a correlation between the inflationary predictions and the $\mathrm{U}(1)_X$ gauge coupling. With this correlation, we have investigated complementarities between the inflationary predictions and the current constraint from the Z' boson resonance search at the LHC Run 2 as well as the prospect of the search for the Z' boson and the right-handed neutrinos at the future collider experiments. For completion of our inflation scenario, we have considered a reheating scenario due to the inflaton decay through the SM Higgs boson, and found the reheating temperature to be sufficiently high.

Here, we comment on the stability of the scalar potential during inflation. We have considered the inflation trajectory in the direction of ϕ with $H = 0$. For $\phi \gg v_\phi$, the scalar potential is approximated by Eq. (13) with replacing the quartic couplings at the tree level by their RG running couplings. If $\lambda_{\rm mix} > 0$ during inflation, we can see a problem that the inflaton potential is destabilized in the SM Higgs direction. In Ref. [8], the authors have shown the numerical result of RG evolution of $\lambda_{\rm mix}$ from the 1 TeV scale to Planck scale, from which we can see that the $\lambda_{\rm mix}$ quickly changes its sign around 1 TeV in the RG evolution. We can easily see this behavior from the RG equation for $\lambda_{\rm mix}$ at one-loop level, which is approximately given by [8]

$$\phi \frac{d\lambda_{\rm mix}}{d\phi} \simeq -\frac{1}{16\pi^2} 12 x_H^2 g_X^4, \tag{37}$$

for $|x_H| \gg 1$. Since the beta function is negative and its absolute value is greater than the initial value of $\lambda_{\rm mix}$ at the TeV scale, we can see that $\lambda_{\rm mix}$ quickly becomes negative in its running. Although the beta function formula becomes very complicated (see [8] for complete formulas) for a small $|x_H|$ value, we obtain the same consequence.

In our analysis we have considered the number of e-folds to be a free parameter and have fixed $N_0 = 60$. However, the number of e-folds is determined by the reheating temperature T_R, and the inflaton potential energy at the horizon exit ($V_E|_{k_0}$) as (see, for example, Ref. [33])

$$N_0 \simeq 51.4 + \frac{2}{3}\ln\left(\frac{V_E|_{k_0}^{1/4}}{10^{15}\ \mathrm{GeV}}\right) + \frac{1}{3}\ln\left(\frac{T_R}{10^7\ \mathrm{GeV}}\right). \quad (38)$$

Because of this relation, the number of e-folds is not a free parameter and is determined as a function of ξ, x_H, and $m_{Z'}$. Using this relation we can make our predictions more precise. However, in such an analysis the inflationary predictions, low energy observables, and reheating temperature are related with each other in a very complicated way through the free parameters ξ, x_H, and $m_{Z'}$. To keep our discussion very clear we have treated N_0 as a free parameter. From Eq. (38), we can see that the true value of N_0 lies in between 50 and 60. As shown in Table I, the inflationary predictions for a fixed ξ weakly depend on N_0 values. Hence our results with $N_0 = 60$ well approximate the true values.

ACKNOWLEDGMENTS

The work of S. O. and D.-s. T. is supported by the mathematical and theoretical physics unit (Hikami unit) and advanced medical instrumentation unit (Sugawara unit), respectively, of the Okinawa Institute of Science and Technology Graduate University. The work of N. O. is supported in part by the United States Department of Energy (Award No. DE-SC0012447).

[1] A. A. Starobinsky, A new type of isotropic cosmological models without singularity, Phys. Lett. **91B**, 99 (1980); A. H. Guth, The inflationary universe: A possible solution to the horizon and flatness problems, Phys. Rev. D **23**, 347 (1981); A. Albrecht and P. J. Steinhardt, Cosmology for Grand Unified Theories with Radiatively Induced Symmetry Breaking, Phys. Rev. Lett. **48**, 1220 (1982); A. D. Linde, Chaotic inflation, Phys. Lett. **129B**, 177 (1983).

[2] P. A. R. Ade *et al.* (Planck Collaboration), Planck 2015 results. XIII. Cosmological parameters, Astron. Astrophys. **594**, A13 (2016).

[3] See, for example, N. Okada, M. U. Rehman, and Q. Shafi, Tensor-to-scalar ratio in nonminimal ϕ^4 inflation, Phys. Rev. D **82**, 043502 (2010); N. Okada, V. N. Senoguz, and Q. Shafi, The observational status of simple inflationary models: An update, Turk. J. Phys. **40**, 150 (2016).

[4] F. L. Bezrukov and M. Shaposhnikov, The standard model Higgs boson as the inflaton, Phys. Lett. B **659**, 703 (2008); J. Garcia-Bellido, D. G. Figueroa, and J. Rubio, Preheating in the standard model with the Higgs-inflaton coupled to gravity, Phys. Rev. D **79**, 063531 (2009); F. Bezrukov, D. Gorbunov, and M. Shaposhnikov, On initial conditions for the hot big bang, J. Cosmol. Astropart. Phys. 06 (2009) 029; F. L. Bezrukov, A. Magnin, and M. Shaposhnikov, Standard model Higgs boson mass from inflation, Phys. Lett. B **675**, 88 (2009); F. Bezrukov and M. Shaposhnikov, Standard model Higgs boson mass from inflation: Two loop analysis, J. High Energy Phys. 07 (2009) 089; F. Bezrukov, A. Magnin, M. Shaposhnikov, and S. Sibiryakov, Higgs inflation: Consistency and generalisations, J. High Energy Phys. 01 (2011) 016; F. Bezrukov and M. Shaposhnikov, Higgs inflation at the critical point, Phys. Lett. B **734**, 249 (2014); Y. Hamada, H. Kawai, K. y. Oda, and S. C. Park, Higgs Inflation is Still Alive after the Results from BICEP2, Phys. Rev. Lett. **112**, 241301 (2014).

[5] A. O. Barvinsky, A. Y. Kamenshchik, and A. A. Starobinsky, Inflation scenario via the standard model Higgs boson and LHC, J. Cosmol. Astropart. Phys. 11 (2008) 021; A. O. Barvinsky, A. Y. Kamenshchik, C. Kiefer, A. A. Starobinsky, and C. Steinwachs, Asymptotic freedom in inflationary cosmology with a nonminimally coupled Higgs field, J. Cosmol. Astropart. Phys. 12 (**2009**) 003; A. O. Barvinsky, A. Y. Kamenshchik, C. Kiefer, A. A. Starobinsky, and C. Steinwachs, Higgs boson, renormalization group, and naturalness in cosmology, Eur. Phys. J. C **72**, 2219 (2012).

[6] A. De Simone, M. P. Hertzberg, and F. Wilczek, Running inflation in the standard model, Phys. Lett. B **678**, 1 (2009); T. E. Clark, B. Liu, S. T. Love, and T. ter Veldhuis, The standard model Higgs boson-inflaton and dark matter, Phys. Rev. D **80**, 075019 (2009).

[7] R. N. Lerner and J. McDonald, Gauge singlet scalar as inflaton and thermal relic dark matter, Phys. Rev. D **80**, 123507 (2009); N. Okada and Q. Shafi, WIMP dark matter inflation with observable gravity waves, Phys. Rev. D **84**, 043533 (2011); K. Mukaida and K. Nakayama, Dark matter chaotic inflation in light of BICEP2, J. Cosmol. Astropart. Phys. 08 (2014) 062; M. Bastero-Gil, R. Cerezo, and J. G. Rosa, Inflaton dark matter from incomplete decay, Phys. Rev. D **93**, 103531 (2016); R. Daido, F. Takahashi, and W. Yin, The ALP miracle: Unified inflaton and dark matter, J. Cosmol. Astropart. Phys. 05 (**2017**) 044; S. Choubey and A. Kumar, Inflation and dark matter in the inert doublet model, J. High Energy Phys. 11 (2017) 080.

[8] S. Oda, N. Okada, and D. s. Takahashi, Classically conformal U(1)' extended standard model and Higgs vacuum stability, Phys. Rev. D **92**, 015026 (2015); A. Das, S. Oda, N. Okada, and D. s. Takahashi, Classically conformal U(1)' extended standard model, electroweak vacuum stability, and LHC Run 2 bounds, Phys. Rev. D **93**, 115038 (2016).

[9] R. N. Mohapatra and R. E. Marshak, Local B-L Symmetry of Electroweak Interactions, Majorana Neutrinos, and Neutron Oscillations, Phys. Rev. Lett. **44**, 1316 (1980); R. N. Mohapatra and R. E. Marshak, Erratum, Phys. Rev. Lett. **44**, 1644 (1980); R. N. Mohapatra and R. E. Marshak, Quark-lepton symmetry and B-L as the U(1) generator of the electroweak symmetry group, Phys. Lett. **91B**, 222 (1980); C. Wetterich, Neutrino masses and the scale of B-L violation, Nucl. Phys. **B187**, 343 (1981); A. Masiero,

J. F. Nieves, and T. Yanagida, $B^{-}l$ violating proton decay and late cosmological baryon production, Phys. Lett. **116B**, 11 (1982); R. N. Mohapatra and G. Senjanovic, Spontaneous breaking of global $B^{-}l$ symmetry and matter-antimatter oscillations in grand unified theories, Phys. Rev. D **27**, 254 (1983); W. Buchmuller, C. Greub, and P. Minkowski, Neutrino masses, neutral vector bosons, and the scale of B-L breaking, Phys. Lett. B **267**, 395 (1991).

[10] T. Appelquist, B. A. Dobrescu, and A. R. Hopper, Nonexotic neutral gauge bosons, Phys. Rev. D **68**, 035012 (2003).

[11] P. Minkowski, $\mu \to e\gamma$ at a rate of one out of 10^9 muon decays?, Phys. Lett. **67B**, 421 (1977); T. Yanagida, in *Proceedings of the Workshop on the Unified Theory and the Baryon Number in the Universe*, edited by O. Sawada and A. Sugamoto (KEK, Tsukuba, Japan, 1979), p. 95; M. Gell-Mann, P. Ramond, and R. Slansky, *Supergravity*, edited by P. van Nieuwenhuizen *et al.* (North Holland, Amsterdam, 1979), p. 315; S. L. Glashow, in *Proceedings of the 1979 Cargèse Summer Institute on Quarks and Leptons*, edited by M. Lévy *et al.* (Plenum Press, New York, 1980), p. 687; R. N. Mohapatra and G. Senjanović, Neutrino Mass and Spontaneous Parity Violation, Phys. Rev. Lett. **44**, 912 (1980); J. Schechter and J. W. F. Valle, Neutrino masses in $SU(2) \times U(1)$ theories, Phys. Rev. D **22**, 2227 (1980).

[12] W. A. Bardeen, Report No. FERMILAB-CONF-95-391-T.

[13] S. R. Coleman and E. J. Weinberg, Radiative corrections as the origin of spontaneous symmetry breaking, Phys. Rev. D **7**, 1888 (1973).

[14] S. Iso, N. Okada, and Y. Orikasa, Classically conformal $B-L$ extended standard model, Phys. Lett. B **676**, 81 (2009); S. Iso, N. Okada, and Y. Orikasa, The minimal B-L model naturally realized at TeV scale, Phys. Rev. D **80**, 115007 (2009).

[15] G. Aad *et al.* (ATLAS and CMS Collaborations), Measurements of the Higgs boson production and decay rates and constraints on its couplings from a combined ATLAS and CMS analysis of the LHC pp collision data at $\sqrt{s} = 7$ and 8 TeV, J. High Energy Phys. 08 (2016) 045.

[16] LEP, ALEPH, DELPHI, L3, and OPAL Collaborations, LEP Electroweak Working Group, SLD Electroweak Group, and SLD Heavy Flavor Group, A combination of preliminary electroweak measurements and constraints on the standard model, arXiv:0312023.

[17] M. Carena, A. Daleo, B. A. Dobrescu, and T. M. P. Tait, Z' gauge bosons at the Tevatron, Phys. Rev. D **70**, 093009 (2004).

[18] S. Schael *et al.* (ALEPH, DELPHI, L3, OPAL, and LEP Electroweak Collaborations), Electroweak measurements in electron-positron collisions at W-boson-pair energies at LEP, Phys. Rep. **532**, 119 (2013).

[19] J. Heeck, Unbroken $B-L$ symmetry, Phys. Lett. B **739**, 256 (2014).

[20] For a review, see M. Sher, Electroweak Higgs potentials and vacuum stability, Phys. Rep. **179**, 273 (1989).

[21] C. P. Burgess, H. M. Lee, and M. Trott, Power-counting and the validity of the classical approximation during inflation, J. High Energy Phys. 09 (2009) 103; C. P. Burgess, H. M. Lee, and M. Trott, Comment on Higgs inflation and naturalness, J. High Energy Phys. 07 (2010) 007; J. L. F. Barbon and J. R. Espinosa, On the naturalness of Higgs inflation, Phys. Rev. D **79**, 081302 (2009); M. P. Hertzberg, On inflation with nonminimal coupling, J. High Energy Phys. 11 (2010) 023.

[22] M. Aaboud *et al.* (ATLAS Collaboration), Search for new high-mass phenomena in the dilepton final state using 36 fb^{-1} of proton-proton collision data at $\sqrt{s} = 13$ TeV with the ATLAS detector, J. High Energy Phys. 10 (2017) 182.

[23] ATLAS Collaboration, Report No. ATLAS-CONF-2016-045.

[24] CMS Collaboration, Report No. CMS-PAS-EXO-16-031.

[25] J. Pumplin, D. R. Stump, J. Huston, H. L. Lai, P. M. Nadolsky, and W. K. Tung, New generation of parton distributions with uncertainties from global QCD analysis, J. High Energy Phys. 07 (2002) 012.

[26] N. Okada and S. Okada, Z'_{BL} portal dark matter and LHC Run 2 results, Phys. Rev. D **93**, 075003 (2016); N. Okada and S. Okada, Z'-portal right-handed neutrino dark matter in the minimal $U(1)_X$ extended standard model, Phys. Rev. D **95**, 035025 (2017).

[27] N. Okada, S. Okada, and D. Raut, Inflection-point inflation in hypercharge oriented $U(1)_X$ model, Phys. Rev. D **95**, 055030 (2017).

[28] D. Buttazzo, G. Degrassi, P. P. Giardino, G. F. Giudice, F. Sala, A. Salvio, and A. Strumia, Investigating the near criticality of the Higgs boson, J. High Energy Phys. 12 (2013) 089.

[29] B. Batell, M. Pospelov, and B. Shuve, Shedding light on neutrino masses with dark forces, J. High Energy Phys. 08 (2016) 052.

[30] B. Schmidt, The high-luminosity upgrade of the LHC: Physics and technology challenges for the accelerator and the experiments, J. Phys. Conf. Ser. **706**, 022002 (2016).

[31] M. Anelli *et al.* (SHiP Collaboration), A facility to Search for Hidden Particles (SHiP) at the CERN SPS, arXiv:1504.04956.

[32] R. Aaij *et al.* (LHCb Collaboration), Search for dark photons produced in 13 TeV pp collisions, arXiv:1710.02867; P. Ilten, Y. Soreq, M. Williams, and W. Xue, Serendipity in dark photon searches, arXiv:1801.04847.

[33] D. H. Lyth and A. Riotto, Particle physics models of inflation and the cosmological density perturbation, Phys. Rep. **314**, 1 (1999).